Monolithic Multi-Scale Modeling of MR-Induced Pacemaker Lead Heating

O. Talcoth* T. Rylander* H. S. Lui* M. Persson*

Abstract — **Modeling of MR-induced pacemaker lead heating is complicated by, among other things, the multi-scale characteristics of the problem. In this paper, the method of moments is used to model a wide range of length scales of the problem simultaneously including the helix-shaped conducting wires present in the pacemaker lead. A cross-section area conserving meshing scheme for helices is proposed and evaluated. For a relative error of 1 %, the meshing scheme reduces the number of thin wire segments needed to model a helix with a factor of roughly 3 to 6, as compared to the conventional approach. In addition, we study the relationship between the maximum induced current on the lead and the number of turns of the helices.**

1 INTRODUCTION

Magnetic resonance imaging (MRI) is the imaging modality of choice in healthcare for imaging of soft tissue and its use in clinics is continuously increasing. Concurrently, active implantable medical devices, such as pacemakers, are being used more frequently. Unfortunately, these implants constitute a contraindication for MRI, which prohibits patients with this type of device from accessing the benefits of MRI. Hence, there is a need for MR safe pacemakers.

The major safety issue for pacemakers during MRI is tissue heating near the electrodes of the pacemaker lead. The lead functions as a receiving antenna for the radio frequency (RF) field of the MRI machine. The induced currents accumulate charge at the electrodes and cause high electric field strengths in the tissue close to the electrode, which causes heating in the electrode vicinity.

Apart from the difficulties created by inter-patient variations in factors like body size, body composition and implant configuration, modeling of this phenomenon includes two major complications. First, this is a multi-scale problem with length scales that differ by several orders of magnitude, such as the size of the MRI system's birdcage coil in comparison to the components of the pacemaker lead. Second, the human body is highly inhomogenous with large variations in its dielectric properties.

Previously, Neufeld et al. [1] employed a two-step approach with the finite-difference time-domain (FDTD) technique to investigate the heating behavior of a single helix-shaped conductor. Although the inhomogeneous nature of human tissue can be easily handled with the FDTD scheme, modeling of modern pacing leads, which often comprise two helix-shaped conducting wires consisting of several sub-wires each, is impossible with this technique in practice due to excessive simulation times.

An alternative method, the method of moments (MoM), was used by Park et al. [2] who simulated MR-induced heating near straight wires, and Bottomley et al. [3] who compared the heating performance of different lead designs. Neither of these studies modeled the finer details of pacemaker leads, which have been experimentally shown to strongly influence the heating generated around the lead tip [3]. Thus, there is a need for more detailed modeling.

In order to overcome the limitations of the aforementioned studies regarding the multi-scale feature of the problem, we use the MoM to model a wide range of the problem geometry length scales simultaneously. Furthermore, we propose and evaluate a meshing scheme for helices that drastically reduces the number of segments needed to resolve the helix for a given level of the discretization error.

2 MODELING

We model the RF electromagnetic fields of a generic 1.5 T MRI system and their interaction with an implanted pacemaker lead. The modeling is performed with the frequency domain MoM implemented in the commercial software Efield® [4].

The modeled geometry is inspired by the test standard ASTM F2182-09 [5] and includes a generic birdcage coil which is monochromatically excited at 64 MHz, and a patient-mimicking phantom with an implanted bi-polar pacemaker lead. The geometry can be seen in figure 1 and each part of it is explained below.

A generic 16-rung birdcage coil with a length and diameter of 0.6 m is modeled by infinitely thin strips of width 0.65 cm that are discretized by triangles. A perfect electric conductor (PEC) material is as-

*Department of Signals and Systems, Chalmers University of Technology, SE-412 96 Göteborg, Sweden, e-mail: {oskar.talcoth; rylander; antony.lui; mikael.persson}@chalmers.se, tel.: +46 31 772 {5186; 1735; 3382; 1576}, fax: +46 31 7721573.

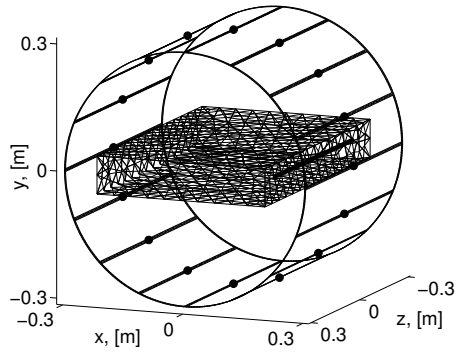

Figure 1: The problem geometry with a 16-rung MRI birdcage coil and a patient-mimicking phantom with an implanted bi-polar pacemaker lead. The sources are marked with spheres.

signed to the coil. The coil is excited by a voltage source at the middle of each rung. The sources have unity amplitude and a linear phase variation of 2π around the birdcage circumference. The currents on the birdcage yield an approximately uniform magnetic field inside the coil, which is desired for the MRI equipment to function.

A head-less phantom from the ASTM standard [5] is used in the model. The phantom is block-shaped with a size of $42\,\mathrm{cm} \times 9\,\mathrm{cm} \times 65\,\mathrm{cm}$ and it is centered in the birdcage coil. The phantom consists of a homogeneous lossy dielectric ($\varepsilon_r = 80$, $\sigma = 0.5\,\mathrm{S/m}$) that models average human tissue at 64 MHz. The maximum element size of the surface mesh is $\lambda/20$.

The implanted bi-polar pacemaker lead is modeled by two conducting wires with a wire diameter of 0.05 mm, that are shaped as two coaxial helices of different diameters, 1 mm for the outer helix and 0.5 mm for the inner helix respectively. Both helices are identical with respect to the orientation of the turns, the overall length of the helix, and the total number of turns. These helices are discretized by straight wire segments using the thin-wire approximation. Consequently, the current on the helix is forced to be aligned with the wire and, thus, its component along the circumference of the wire is set to zero. This representation of the current cannot be expected to be accurate for densly wound helices.

The lead is straight and parallel to the cylinder axis of the birdcage coil. It is displaced from the symmetry axis such that its mid-point is located at $(18, 0, 5)\,\mathrm{cm}$, as shown in figure 1. Thus, the lead is located at a distance of 3 cm from the phantom surface in the x-direction.

3 MESHING WITH AREA COMPENSATION

The thin-wire approximation of a helix employed by our modeling approximates one turn of the helix by N equally long wire segments. A simple meshing approach exploits N uniformly placed points on each helix turn and connects them with straight line segments. However, for a small number of line segments the cross-section area of the discretized helix is significantly smaller than the area of the original helix. The cross-section area is an important characteristic of solenoidal coils at low frequencies and influences, for example, the inductance. Therefore, we propose a meshing scheme that preserves the cross-section area by scaling the radius of the discretized helix. A mesh convergence study is used to evaluate the performance of the proposed meshing scheme in comparison with the simple meshing scheme.

The area, A_{poly}, of a N-sided regular polygon inscribed in a circle with radius $\tilde{r}$ is given by $A_{\mathrm{poly}} = (N\tilde{r}^2/2)\sin(2\pi/N)$. In order to obtain a polygon with the same area as a circle of radius r, we equate the area of the polygon with the area of the circle and solve for $\tilde{r}$ to obtain the area compensated radius

$$\tilde{r} = r\sqrt{\frac{2\pi/N}{\sin(2\pi/N)}}. \qquad (1)$$

Whereas the simple meshing approach exploits N points per turn for the helix of radius r, the proposed scheme instead uses the same number of points from a helix of radius $\tilde{r}$. The difference between the two meshing schemes is illustrated in figure 2 for $N = 4$.

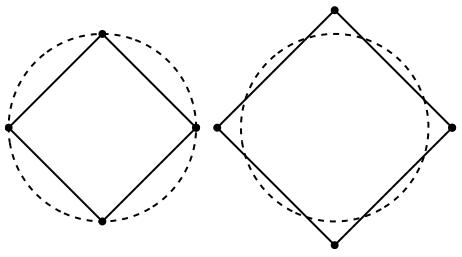

Figure 2: Meshing without (*left*), and with (*right*) area compensation.

We perform a convergence study for four 0.2 m long helices: (i) a single helix in air, (ii) a double helix in air, (iii) a single helix in the phantom, and (iv) a double helix in the phantom. For the helices in air, we use an incident plane wave that (i) propagates in a direction perpendicular to the helix axis

and (ii) features a polarization parallel to the helix axis. The frequency of the plane wave is multiplied by $\sqrt{\varepsilon_r}$ to make the electrical size of the lead in air equal to the electrical size of the lead in the dielectric phantom. The mesh is refined in a hierarchical way by varying the number of segments per helical turn. The first mesh node from each turn of the coarsest mesh is present in all the refined meshes.

The induced complex current $\mathbf{j}_k$ on the lead is modeled by

$$\mathbf{j}_k^{\text{model}}(N,p) = \mathbf{a}_k(p) + \mathbf{b}_k(p)N^{-p} + \dots \quad (2)$$

for all $k \in \kappa(N)$, where k is the node number, N is the number of segments per helix turn, $\kappa(N)$ is the set of nodes present in all meshes, and $\mathbf{a}_k(p)$ and $\mathbf{b}_k(p)$ are complex constants. We subsequently neglect the higher order terms and apply the following optimization approach to find the order of convergence, p. First, a number of candidate values for p are chosen. Then, for each of these candidate values the constants $\mathbf{a}_k(p)$ and $\mathbf{b}_k(p)$ are computed by solving equation (3) in the least-squares sense, where $\mathbf{j}_k^{\text{sim}}(N)$ is the current from the simulations, i.e.

$$\mathbf{j}_k^{\text{sim}}(N) = \mathbf{a}_k(p) + \mathbf{b}_k(p)N^{-p}. \quad (3)$$

Finally, the order of convergence, $p^\star$, is found as the candidate value that minimizes the total error according to equation (4), where ν is the set of investigated values for N.

$$p^\star = \arg\min_p \sqrt{\sum_{N\in\nu}\sum_{k\in\kappa(N)} \left|\mathbf{j}_k^{\text{model}}(N,p) - \mathbf{j}_k^{\text{sim}}(N)\right|^2} \quad (4)$$

In our study, we exclude the coarser meshes from the sum over N in equation (4) to ensure that only values from the region of convergence according to equation (3) are used and to obtain good agreement between the model and the data. This results in $\nu = \{12, 16, 20, \dots, 32\}$ for the simple meshing scheme and $\nu = \{5, 6, 7\}$ for the proposed meshing scheme.

The relative error, $\rho(N)$, is computed according to equation (5) where the values $\mathbf{a}_k(p^\star)$ for the simple meshing scheme are used as a reference. These values correspond to the extrapolation to zero cell size of the current, i.e. let $N \to \infty$ in equation (2), and are also used as reference for the proposed meshing scheme.

$$\rho(N) = \frac{\sqrt{\sum_k \left|\mathbf{j}_k^{\text{sim}}(N) - \mathbf{a}_k(p^\star)\right|^2}}{\sqrt{\sum_k \left|\mathbf{a}_k(p^\star)\right|^2}} \quad (5)$$

The relative error for a single helix in air, with and without area compensation, is given in figure 3 as a function of the number of segments per turn N. Clearly, the proposed meshing scheme has a higher order of convergence and a smaller error than the simple scheme. The estimated orders of convergence, as well as the number of segments needed per turn to obtain a relative error smaller than 1 %, are given in table 1 for the four test cases. The proposed meshing scheme reduces the number of wire segments needed with a factor between 3.0 and 5.9 depending on the type of simulation. Hence, the proposed meshing scheme makes larger problem sizes amenable for a specified error, or conversely, more accurate results are obtained at a specified problem size.

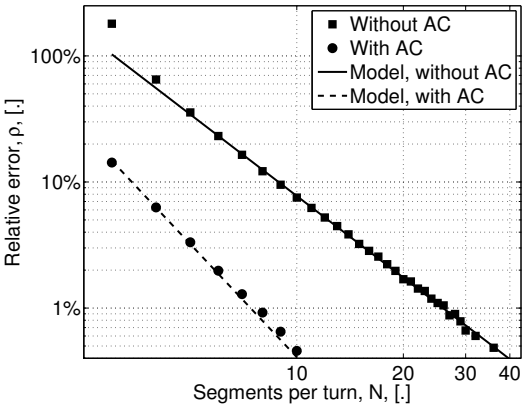

Figure 3: Relative error, with and without area compensation (AC), for a single helix in air, as a function of the number of segments per turn, N.

Case	Simple $p^\star$	Simple $N_{\rho<1\%}$	Proposed $p^\star$	Proposed $N_{\rho<1\%}$
Air, single	2.15	27	2.98	8
Air, double	1.72	65	3.64	11
Phantom, single	2.08	19	3.10	6
Phantom, double	1.92	15	3.36	5

Table 1: Order of convergence for the two meshing schemes and the number of segments needed per turn to obtain a relative error smaller than 1 % for the four test cases.

4 INFLUENCE OF THE NUMBER OF TURNS

In a low-frequency setting, the inductance per unit length of a solenoidal coil is proportional to the square of the number of turns per unit length. Here, we perform a parameter study to establish a relationship between the maximum induced current on

a 0.5 m double helix inside the phantom and the number of turns of the helix. We exploit the meshing scheme with area compensation for eight segments per turn. The inner and outer helix have the same number of turns which is varied in the study. Furthermore, the inner and outer helices are modeled separately to investigate the interactions between them in the context of forming a double helix. In all results below, the power has been scaled to a whole-body averaged SAR of 1 W/kg with the lead in place by assuming that the phantom has the density of water.

Figure 4 shows the maximum amplitude of the induced current on the helices for different number of turns. As seen in the figure, the current is lower on the double helix compared to the individually excited helices. Also, the maximum current amplitude is greater on the inner than on the outer helix. The maximum current decreases when the number of turns increases, where contributing factors are an increased inductance per unit length of the helix and changes in the coupling of the incident field to the induced current. It is interesting to notice that, as the number of turns increases and the current on the outer helix decreases, the current on the inner helix (dashed curve with squares) approaches the case where the outer helix is removed (solid curve with squares).

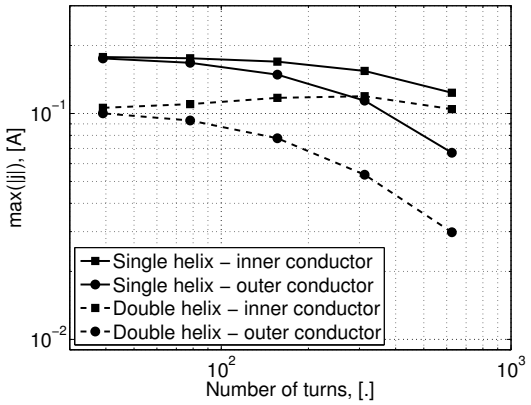

Figure 4: Maximum current amplitude as a function of the number of turns of the helix.

5 CONCLUDING REMARKS

In this paper, the multi-scale problem of pacemaker lead heating in MRI was modeled using the MoM. A meshing scheme for helices that gives the correct cross section area, regardless of the number of segments per turn, was proposed and evaluated. The number of segments required to achieve a discretization error of 1 % was reduced with a factor of roughly 3 to 6 by the proposed meshing scheme. This is highly beneficial since the memory usage of the MoM is proportional to n^2, and the number of floating-point operations is proportional to n^3, where n is the number of unknowns.

Additionally, the meshing scheme was employed to study the impact of the number of turns on the maximum current induced on a double helix. The current was smaller on the double helix than on its individual helices when excited individually. Furthermore, the current was larger on the inner helix than on the outer helix and decreased with an increased number of turns.

The heating at the lead electrodes is due to strong electric fields which are related to the accumulated charge at the electrodes. Thus, the charge would be a relevant quantity to compute and analyze from the simulations. However, in our present model the electrodes are represented by the ends of thin wires, a representation that is quite different from the underlying physical problem. Our future work therefore includes the development of more realistic models of the electrodes.

Acknowledgments

This work has been supported by the Swedish research council VINNOVA via a project within the VINN Excellence center CHASE, and by the Swedish National Graduate School in Scientific Computing. The computations were performed on C3SE computing resources at Chalmers University of Technology in Göteborg, Sweden.

References

[1] E. Neufeld, S. Kühn, G. Szekely, and N. Kuster, "Measurement, simulation and uncertainty assessment of implant heating during MRI.", Phys. Med. Bio., Vol. 54, No. 13, pp 4151-4169, 2009.

[2] Park, S.M., R. Kamondetdacha, and J.A. Nyenhuis. "Calculation of MRI-induced heating of an implanted medical lead wire with an electric field transfer function.", J. Magn. Reson. Imaging, Vol. 26, No. 5, pp 12781285, 2007.

[3] P. Bottomley, A. Kumar, W. Edelstein, J. Allen, and P. Karmarkar. "Designing passive MRI-safe implantable conducting leads with electrodes." Medical Physics, Vol. 37, No. 7, pp 3828-3843, 2010.

[4] Efield AB, Stockholm, Sweden, www.efieldsolutions.com

[5] "Standard test method for measurement of radio frequency induced heating on or near passive implants during magnetic resonance imaging", Standard F2182-09. ASTM International, West Conshohocken, PA, USA, 2010.